

Field-Induced Magnetic Transitions in Single Crystals of RZn_2 ($R=Pr, Nd, Dy$)(Magnetism)

著者	Kitai T., Kaneko T., Abe S., Ohashi M., Nakagawa Y.
journal or publication title	Science reports of the Research Institutes, Tohoku University. Ser. A, Physics, chemistry and metallurgy
volume	38
number	2
page range	179-187
year	1993-06-30
URL	http://hdl.handle.net/10097/28434

Field-Induced Magnetic Transitions in Single Crystals of
 RZn_2 ($R = Pr, Nd, Dy$)*

T. Kitai^a , T. Kaneko^b , S. Abe^b,
 M. Ohashi^b and Y. Nakagawa^b

^aDepartment of Applied Physics, Kyushu Institute of Technology,
 Kitakyushu 804

^bInstitute for Materials Research, Tohoku University, Sendai 980

(Received January 18, 1993)

Synopsis

Temperature dependence of magnetic susceptibility and high field magnetism are studied for single crystals of antiferromagnetic compounds $PrZn_2$, $NdZn_2$ and $DyZn_2$. The paramagnetic Curie temperatures are anisotropic and different field-induced transitions are observed along each crystal axis direction.

I. Introduction

Rare earth intermetallic compounds RZn_2 (R =rare earth metals) have the orthorhombic crystal structure of the $CeCu_2$ -type, in which the R atoms occupy the $4e$ and the Zn atoms the $8h$ sites, forming a double-layer structure of R atoms along the c -axis as shown in Figure 1. Magnetic properties of these compounds have been studied by Debray et al.¹⁾⁻⁷⁾ using polycrystalline samples and reported that they are antiferromagnetic except for $GdZn_2$ and $ErZn_2$ and these compounds showed various interesting magnetic behaviors.

The results of $PrZn_2$ ¹⁾ show that the magnetic moment of Pr ion decrease monotonically with increasing temperature and the effective magnetic moment and paramagnetic Curie temperature are $\mu_{eff} = 3.56 \mu_B/Pr$ and $\theta_P = 14$ K, respectively. It is also reported that the compound has no magnetic order down to

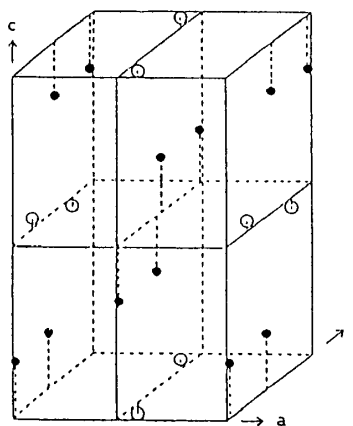


Fig.1. Crystal structure of RZn_2 .
 The open and closed circles indicate the rare earth and zinc atoms.

*The 1919th report of Institute for Materials Research

4.2 K and becomes a van Vleck paramagnet at low temperatures.

For NdZn_2 ^{1), 3)}, the results of neutron diffraction experiments indicate the magnetic structure to be a composite of sinusoidal transverse wave moment alignment polarized in the b-axis and propagation along the c-axis, and ferromagnetic moment along the b-axis. The magnitude of the ordered moment found for Nd is $\sim 2.4 \mu_B$ and is considerably smaller than the free ion value. However, no field-induced antiferromagnetic transition in the magnetization process of a polycrystalline sample in magnetic fields up to 50 kOe has been observed. For DyZn_2 , the results of magnetic measurements on apolycrystalline sample by Debray et al.^{1), 7)} show that DyZn_2 undergoes simply some type of antiferromagnetic ordering below the Neel temperature $T_N=35$ K, where the paramagnetic Curie temperature is +31.5 K and the effective paramagnetic moment is $10.45 \mu_B/\text{Dy}$. Recently, we have carried out neutron diffraction experiments on a polycrystalline sample of DyZn_2 ⁸⁾.

The results reveal that, with decreasing temperature, a linear modulated antiferromagnetic structure (AF2) with (0 0 0.45) develops at 35 K. The first order transition takes place at 29 K, below which DyZn_2 has a commensurably modulated antiferromagnetic structure (AF1) with (0 0 0.5) and the magnetic moment of $9.7 \mu_B/\text{Dy}$ tilts about 16° from the b-axis. The occurrence of an incommensurate magnetic structure and the polarization of magnetic moment of R ion along the b-axis are the common features for the magnetic properties of TbZn_2 ²⁾ and HoZn_2 ⁵⁾ compounds.

In the last few years, we have studied high field magnetism on a single crystal of NdZn_2 ⁸⁾, PrZn_2 ¹¹⁾ and DyZn_2 ¹⁰⁾ under static magnetic field up to 170 kOe and observed complex field-induced magnetic transitions for each direction of the crystal axis. In this paper, we report the high field magnetism of the NdZn_2 , PrZn_2 and DyZn_2 compounds.

II. Experimental Procedure

The single crystals of RZn_2 were prepared by melting together stoichiometric amounts of rare earth metal(3N) and Zn(4N) in a tantalum crucible and subsequently cooling slowly in an electric furnace under argon atmosphere, and annealing at 400 °C for 50 hours. The samples were confirmed to be a single phase of the CeCu_2 type crystal structure by X-ray diffraction

The temperature variation of the magnetic susceptibility was measured using a Faraday type magnetic balance in a magnetic field of 1~5 kOe at temperature from 4.2 K to 300 K. Magnetization measurements were carried out by a vibrating sample magnetometer in a static magnetic field up to 170 kOe, which was generated by a water cooled Bitter type magnet installed in High Field Laboratory for Superconducting Materials, IMR, Tohoku University.

III. Experimental Results and Discussion

3-1. PrZn₂

Figure 2 shows the temperature dependence of the magnetic susceptibilities along the a-, b- and c-axes of the orthorhombic cell of PrZn₂ under a magnetic field of 5 kOe. Both the susceptibilities along the a- and b-axes have remarkable temperature dependence and sharp peaks at 23 K (=T_N) and 10K(=T_m), respectively. The temperature dependence of the susceptibility along the c-axis is small in marked contrast to those along the a- and b-axes and shows a slight anomaly around 20 K.

Figure 3 shows the temperature dependence of reciprocal susceptibilities along the a-, b- and c-axes at temperature far above T_N. As seen in the figure, all the reciprocal susceptibilities followed well the Curie-Weiss law, with the paramagnetic Curie temperatures, $\theta_a = 16.9$ K along the a-axis, $\theta_b = 2.9$ K along the b-axis and $\theta_c = -72.5$ K along the c-axis. The effective magnetic moment was found to be $3.7 \mu_B/\text{Pr}$, which is in good agreement with the value of $3.58 \mu_B$ for the Pr³⁺ free ion.

Figure 4 shows the magnetization curves along the a-axis at 6 K (below T_m), 15 K (between T_m and T_N) and 20 K (near T_N). The magnetization at 6 K increases linearly with the field at first, shows a discontinuous increase at 17 kOe(= H_{t_a}), and appears to be saturated above 60 kOe. The value of the magnetization at 170 kOe is 64 emu/g, giving the magnetic moment of Pr ion, $\mu_{\text{Pr}} = 3.1 \mu_B$, which agrees well

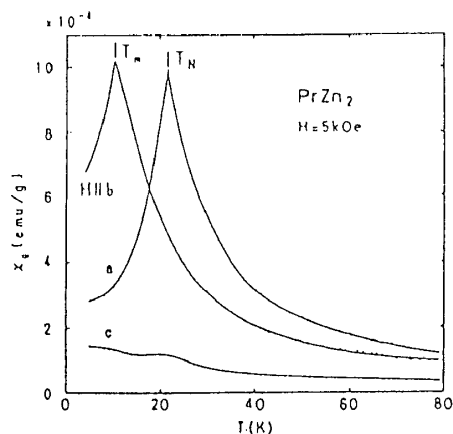


Fig. 2. Temperature dependence of magnetic susceptibilities along the a-, b- and c-axe of PrZn₂.

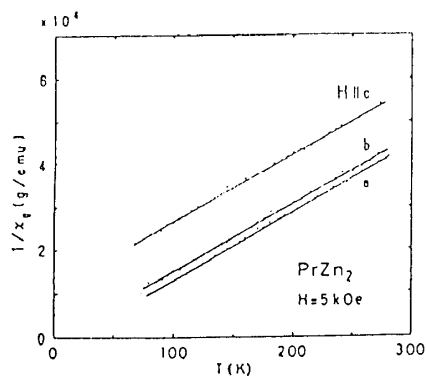


Fig. 3. Temperature dependence of the reciprocal magnetic susceptibilities along the a-, b- and c-axes of PrZn₂.

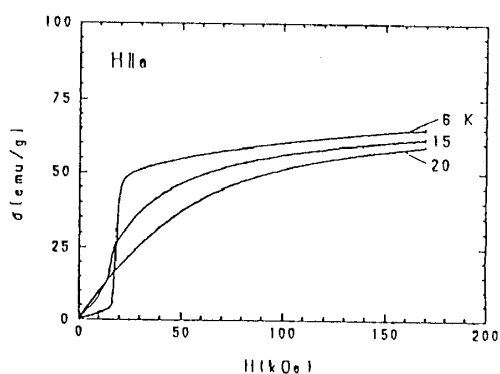


Fig. 4. Magnetization curves along the a-axis of PrZn₂ at 6, 15 and 20 K.

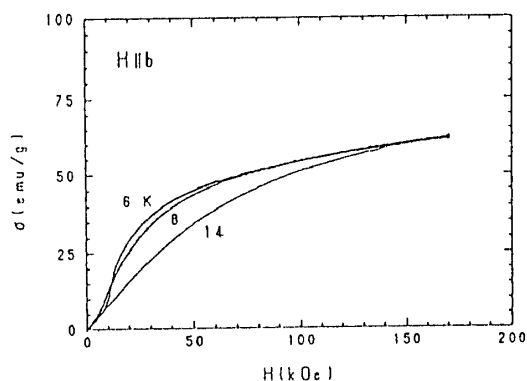


Fig. 5. Magnetization curves along the b-axis of PrZn_2 at 6, 8 and 14 K.

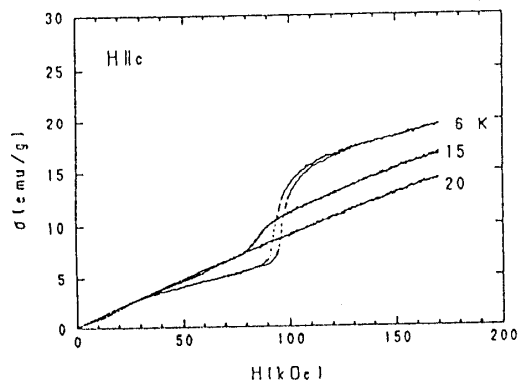


Fig. 6. Magnetization curves along the c-axis of PrZn_2 at 6, 15 and 20 K.

with $3.2 \mu_B$ for Pr^{3+} ion. The abrupt increase of the magnetization at 17 kOe is considered to be due to a field-induced magnetic transition from the antiferromagnetic to the ferromagnetic state. In the magnetizing process at 15 K, a field-induced transition was still observed at 15 kOe, but the magnetization curve at 20 K did not show any significant anomaly.

Figure 5 shows the magnetization curves along the b-axis at 6 and 8 K (below T_m), and 14 K (between T_m and T_N). The magnetization curve at 6 K shows an abrupt increase at about 12 kOe ($=H_{bt}$) and a tendency to saturation above 80 kOe. At 8 K, a steep rise in the magnetization around 8 kOe was also observed, which corresponds to the field-induced transition. This transition was not observed along the b-axis at temperatures above 10 K.

Figure 6 shows the magnetization curves along the c-axis at 6, 15 and 20 K. The magnetization curve at 6 K shows an abrupt increase at 96 kOe ($=H_{ct}$) and a tendency to saturation above 140 kOe. In contrast with the magnetization process along the a- and b-axes, hysteresis at H_{ct} was observed and the value of the magnetization at 170 kOe is much smaller than those along the a- and b-axes. The magnetization anomaly around 30 kOe was dependent on the setting of the sample. At 15 K above T_m , the field-induced transition was still observed, but the magnetization at 20 K increases linearly with field within the magnetic field range employed here. These results suggest that T_m would be the temperature where same kind of magnetic phase change occurs.

3-2 NdZn_2

Figure 7 shows the temperature dependence of magnetic susceptibilities and the inverse ones along the a-, b- and c-axes of NdZn_2 under a magnetic field of 5 kOe and under a magnetic field of 1 kOe along the b-axis. The susceptibilities along the a- and c- axes showed only one sharp peak at 18 K ($=T_{N1}$). The susceptibility along the b-axis under a magnetic field of

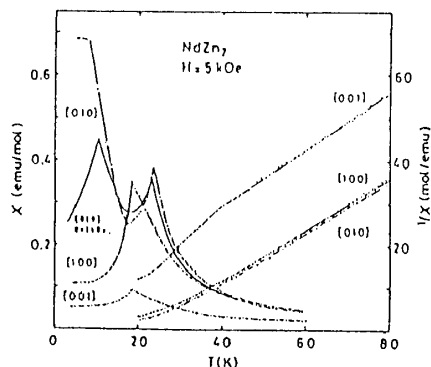


Fig. 7. Temperature dependence of the magnetic susceptibilities and inverse ones along the a-, b- and c-axes of NdZn_2 .

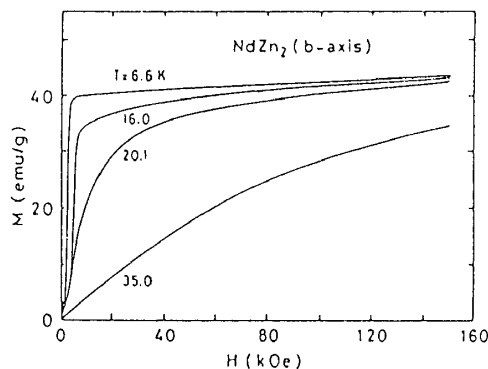


Fig. 8. Magnetization curves along the b-axis of NdZn_2 at various temperatures.

1 kOe showed two peaks at 10 K ($=T_m$) and 23 K (T_{N2}). The magnetic susceptibility along the b-axis in a field of 5 kOe was large below 10 K ($=T_m$) and decreased with the rise of temperature, and it showed a sharp peak at 23 K ($=T_{N2}$). The reciprocal susceptibilities along a-, b- and c-axes at temperature above 60 K obeyed the Curie-Weiss law, with the paramagnetic Curie temperatures along the a-, b- and c-axes, 16.3, 17.5 and -22.7 K, respectively. The effective magnetic moment was found to be $3.8 \mu_B/\text{Nd}$, which is in good agreement with the Nd^{3+} free ion value of $3.6 \mu_B$.

Figure 8 shows the magnetization curves of NdZn_2 along the b-axis at 6.6 K (below T_m), 16 K (between T_m and T_{N1}), 20.1 K (between T_{N1} and T_{N2}) and 35 K (above T_{N2}). The magnetization at 6.6 K increased abruptly at a very low critical field of about 1.5 kOe ($=H_{bt}$) and appears to be saturated. This abrupt increase of the magnetization at H_{bt} is considered to be a field-induced magnetic transition from the sinusoidal magnetic structure to the ferromagnetic one. The saturation moment at 150 kOe is 40 emu/g, giving magnetic moment of $2.0 \mu_B/\text{Nd}$ which is in good agreement with the calculated value of $1.9 \mu_B$ on the basis of the crystalline field parameters estimated from the paramagnetic Curie temperatures. In the temperature range 16-20 K, a field-induced transition was observed at 5 kOe. This critical field was higher than that at 6.6 K and thus, in the temperature range 10-25 K, there is an unknown antiferromagnetic structure different from sinusoidal magnetic structure. This is related to the fact that the susceptibility in 5 kOe is different from that in 1 kOe in the temperature range as shown in Fig. 7.

Figure 9 shows the magnetization curves along the a-axis at 6.4 K, 16.2 K, 20.1 K and 34.8 K. In the magnetization at 6.4 K, a field-induced magnetic transition was observed at 10 kOe ($=H_a$) and at ~ 80 kOe, respectively.

At H_a , sinusoidal moment alignment directed to the b-axis underwent spin-flop transition and increased toward saturation moment $\sim 2 \mu_B/\text{Nd}$

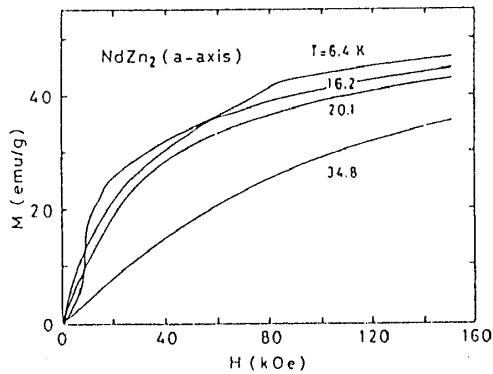


Fig. 9. Magnetization curves along the a-axis of NdZn_2 at various temperatures.

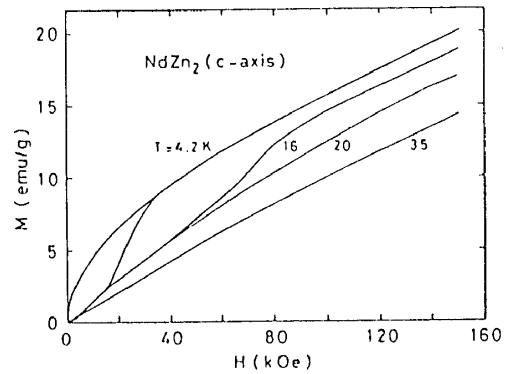


Fig. 10. Magnetization curves along the c-axis of NdZn_2 at various temperatures.

above H_3 . Above 20 K, no transition was observed.

Figure 10 shows the magnetization curves along the c-axis at 4.2 K (below T_m), 16 K (between T_m and T_{N1}), 20 K (between T_{N1} and T_{N2}) and 35 K (above T_{N2}). In the magnetization curves at 4.2 K and 16 K, a field-induced magnetic transition is observed at ~ 8 kOe and ~ 42 kOe, respectively.

It is noticeable that the magnetization curve at 4.2 K shows a large hysteresis and no remanent magnetization.

In a tetragonal crystal field, the ten fold degenerate 4f state of Nd^{3+} ion splits into relatively narrow five doublets state. The crystal field only energy splitting was estimated as about 80 K. There is thus the possibility of mixing energy levels and demonstrating field induced magnetic transitions in a high magnetic field.

3-3 DyZn_2

Figure 11 shows the temperature dependence of the magnetic susceptibilities along the a-, b- and c-axes of a single crystal DyZn_2 under a magnetic field of 3 kOe. All the magnetic susceptibilities have a peak at 38 K ($=T_N$) and show a slight anomaly at 32 K ($=T_t$). The temperatures of the susceptibility peak and anomaly correspond to T_N and T_t observed in neutron diffraction measurements, respectively.

Figure 12 shows the temperature dependence of the reciprocal magnetic susceptibilities along the a-, b- and c-axes at temperature above T_N , which follow well the Curie-Weiss law. The paramagnetic Curie temperatures θ_a , θ_b and θ_c along

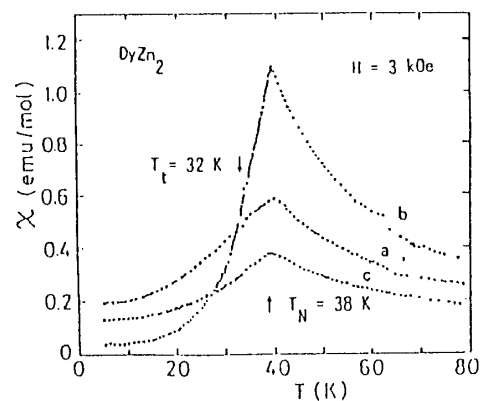


Fig. 11. Temperature dependence of the magnetic susceptibilities along the a-, b- and c- axes of DyZn_2 .

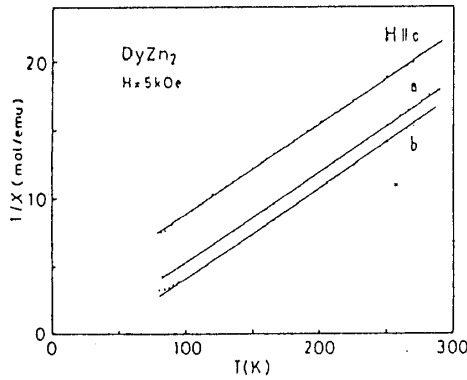


Fig.12. Temperature dependence of the reciprocal magnetic susceptibilities along the a-, b- and c-axes of DyZn_2 .

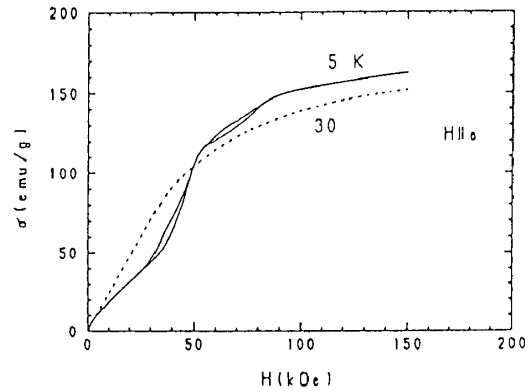


Fig.13. Magnetization curves along the a-axis of DyZn_2 at 5 and 30 K.

the a-, b- and c-axes were 21.0 K, 38.4 K and -35.7 K, respectively. The effective Bohr magneton was $10.9 \mu_B/\text{Dy}$, which agrees with that of a free Dy^{3+} ion.

Figure 13 shows the magnetization curves along the a-axis. A two-stage field-induced transition is observed around 40 kOe ($= H_{a1}$) and 75 kOe ($= H_{a2}$) in a magnetization process at 5 K. Hysteresis in both transitions is observed. It is considered that this transition is not that from the AF1 to the AF2 state, but to an intermediate state, since an extrapolation of the magnetization after the first transition to zero field intersects the magnetization axis at a finite value. The value of the magnetization at 150 kOe is smaller than the saturation magnetization $\sigma^{\text{ND}} = 190 \text{ emu/g}$ estimated from neutron diffraction studies⁹⁾. The transition disappears at 30 K.

Figure 14 shows the magnetization curves along the b-axis. At 5 K, the magnetization increases abruptly at 14 kOe ($= H_{b1}$) and is saturated above about 80 kOe. A large hysteresis is observed at this field-induced transition. This transition corresponds to that from the AF1 to the ferromagnetic state, since the value of the magnetization at 150 kOe is in good agreement with that for σ^{ND} . At 40 K, no transition is observed.

Figure 15 shows the magnetization curves along the c-axis. The numbers in the magnetization curves at 5 K are ordinal numbers of sequential magnetization measurements. As the magnetic field increases, the magnetization increases abruptly at 146 kOe ($= H_{c1}$) (curve (1)) and shows a hysteresis with decreasing field (curve (2)). The curves (3) and (4) are those measured just after the 1st run (1) and (2) of measurements. A two-stage field-induced transition occurs around 40 and 50 kOe. Once the sample is annealed at room temperature, the magnetization process (1) is reproduced. The magnetization curves (3) and (4) have features similar to those along the a-axis, which show a two-stage induced transition around 40 and 75 kOe.

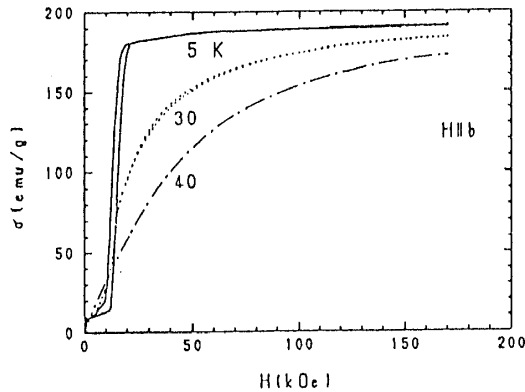


Fig. 14. Magnetization curves along the b-axis of DyZn_2 at 5, 30 and 40 K.

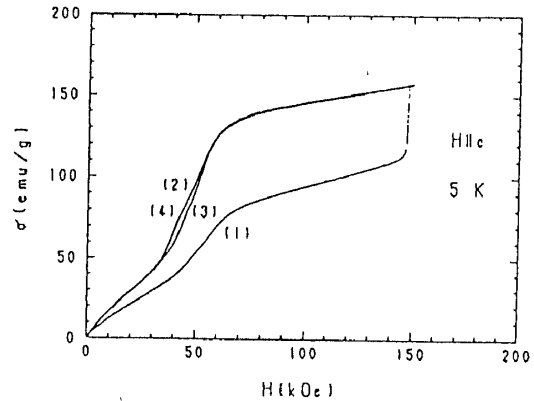


Fig. 15. Magnetization curves along the c-axis of DyZn_2 at 5 K.

As mentioned above, both the a- and c-axes are hard axes and the spin tilts 16° from the b-axis to the c-axis⁹⁾. From the peculiar behavior of the magnetizing process along the c-axis it may be considered that the tilt direction of the spin is changed from the c-axis to the a-axis at H_{bt} and pinned when the high magnetic field is applied along the c-axis. Then the magnetization process similar to those along the a-axis appears after the 1st run of measurements. A similar behavior of the magnetization is observed in DyCu_2 by Hashimoto et al.¹²⁾ and explained qualitatively in terms of a magnetic anisotropy and magnetoelastic energy.

As mentioned above, the results of magnetic measurements on single crystalline samples of PrZn_2 , NdZn_2 and DyZn_2 exhibit peculiar behaviors of the magnetization process along the each direction of the crystal axis.

In particular, the pinning of spin direction observed in DyZn_2 after the field-induced transition occurs.

Acknowledgement

A part of this work was carried out under the Inter-University Cooperative Research Program of IMR, Tohoku University.

References

- 1) D. Debray, W. E. Wallace, and E. Ryba, *J. less-common Metals* 22 (1970) 19
- 2) D. Debray, M. Sougi, and P. Meriel, *J. chem. Phys.* 56 (1972) 4325
- 3) D. Debray and M. Sougi, *J. chem. Phys.* 58 (1973) 1783
- 4) D. Debray *phys. stat. sol. (a)* 18 (1973) 227
- 5) D. Debray and M. Sougi, *J. chem. Phys.* 57 (1972) 2156
- 6) D. Debray and J. Sakurai, *Phys. Rev. B* 9 (1974) 2129
- 7) D. Debray, B. F. Wortmann, and S. Methfessel, *phys. stat. sol. (a)* 30 (1975) 713

- 8) T. Kitai, T. Kaneko, S. Abe, S. Tomiyoshi and Y. Nakagawa, J. Magn. Magn. Mater. 90 & 91 (1990) 55
- 9) M. Ohashi, T. Kitai, T. Kaneko, H. Yoshida, Y. Yamaguchi and S. Abe, J. Magn. Magn. Mater. 90 & 91 (1990) 585
- 10) S. Abe, T. Kaneko, M. Ohashi, Y. Nakagawa and T. Kitai, J. Magn. Magn. Mater. 104-107 (1992) 1403
- 11) T. Kaneko, T. Kitai, S. Abe, M. Ohashi and Y. Nakagawa, Physica B 177 (1992) 295
- 12) Y. Hashimoto, A. Yamagishi, T. Takeuchi and M. Date, J. Magn. Magn. Mater. 90 & 91 (1990) 49